Spectral evolution with incremental nanocoating of long period fiber gratings

Ignacio Del Villar, Jesus M. Corres, Miguel Achaerandio, Francisco J. Arregui and Ignacio R. Matias

Departamento de Ingeniería Eléctrica y Electrónica, Universidad Pública de Navarra, 31006 Pamplona, Spain.
ignacio.delvillar@unavarra.es

Abstract: The incremental deposition of a thin overlay on the cladding of a long-period fiber grating (LPFG) induces important resonance wavelength shifts in the transmission spectrum. The phenomenon is proved theoretically with a vectorial method based on hybrid modes and coupled mode theory, and experimentally with electrostatic self-assembly monolayer process. The phenomenon is repeated periodically for specific overlay thickness values with the particularity that the shape of the resonance wavelength shift depends on the thickness of the overlay. The main applications are the design of wide optical filters and multiparameter sensing devices.

OCIS codes: (050.2770) Gratings, (060.2370) Fiber optics sensors (260.2110), Electromagnetic theory, (310.1860) Deposition and fabrication.

References and links

1. V. Bhatia, "Applications of long-period gratings to single and multi-parameter sensing," Opt. Express **4**, 457-466 (1999).
2. S. W. James and R. P. Tatam, "Optical fibre long-period grating sensors: characteristics and application," Meas. Sci Technol. **14**, R49-R61 (2003).
3. J. R.Qiang and H. E. Chen, "Gain flattening fibre filters using phase shifted long period fibre grating," Electron. Lett. **34**, 1132-1133 (1998).
4. A. M. Vengsarkar, P. J. Lemaire, J. B. Judkins, V. Bhatia, T. Erdogan, and J. E. Sipe, "Long-period fiber gratings as Band Rejection Filters," J. Lightwave Technol. **14**, 58-65 (1996).
5. B. J. Eggleton, R. E. Slusher, J. B. Judkins, J. B. Stark and A. M. Vengsarkar, "All-optical switching in long period fiber gratings," Opt. Lett. **22**, 883-885 (1997).
6. N. D. Rees, S. W. James, R. P. Tatam and G. J. Ashwell, "Optical fiber long-period gratings with Langmuir-Blodgett thin-film overlays," Opt. Lett. **27**, 686-688 (2002).
7. I. Del Villar, M. Achaerandio, I. R. Matias and F. J. Arregui, "Deposition of an Overlay with Electrostactic Self-Assembly Method in Long Period Fiber Gratings," Opt. Lett. **30**, 720-722 (2005).
8. I. Del Villar, I. R. Matias, F. J. Arregui and M. Achaerandio, "Nanodeposition of materials with complex refractive index in long-period fiber gratings," J. Lightwave Technol. 2**3**, 4192-4199 (2005).
9. Z. Y. Wang, J. R. Heflin, R. H. Stolen, S. Ramachandran, "Analysis of optical response of long period fiber gratings to nm-thick thin-film coatings," Opt. Express **13**, 2808-2813 (2005).
10. D. W. Kim, Y. Zhang, K. L. Cooper and A. Wang, "Fibre-optic interferometric immuno-sensor using long period grating," Electron. Lett. **21**, 324-325 (2006).
11. Q. Chen, J. Lee, M. R. Lin, Y. Wang, S. S. Yin, Q. M. Zhang and K. A. Reichard "Investigation of tuning characteristics of electrically tunable long-period gratings with a precise four-layer model," J. Lightwave Technol. **24**, 2954-2962 (2006).
12. A. Cusano, A. Iadicicco, P. Pilla, L. Contesta, S. Campopiano, A. Cutolo, and M. Giordano, "Mode transition in high refractive index coated long period gratings," Opt. Express **14**, 19-34 (2006).
13. P. Pilla, A. Iadicicco, L. Contesta, S. Campopiano, A. Cutolo, M. Giordano, G. Guerra and A. Cusano, "Optical chemo-sensor based on long-period gratings coated with δ form syndiotactic polystyrene," IEEE Photon. Technol. Lett. **17**, 1713-1715, (2005).
14. I. Del Villar, I. R. Matias, F. J. Arregui and P. Lalanne, "Optimization of sensitivity in long period gratings with overlay deposition," Opt. Express **13**, 56-69 (2005).
15. I. Del Villar, I. R. Matias and F. J. Arregui, "Influence on cladding mode distribution of overlay deposition on long-period fiber gratings," J. Opt. Soc. Am. A, **23**, 651-658 (2006).

#74595 - $15.00 USD Received 11 September 2006; revised 31 October 2006; accepted 31 October 2006

16. E. Anemogiannis, E. N. Glytsis and T. K. Gaylord, "Transmission characteristics of long- period fiber gratings having arbitrary azimutal/radial refractive index variation," J. Lightwave Technol., **21**, 218-227, (2003).
17. T. Erdogan, "Cladding-mode resonances in short- and long- period fiber grating filters," J. Opt. Soc. Am. A, **14**, 1760-1773 (1997).
18. S. Guo, S. Albin and S. Rogowski, "Comparative analysis of Bragg fibers," Opt. Express **12**, 198-207 (2004).
19. I. Del Villar, I. R. Matias and F. J. Arregui, "Enhancement of sensitivity in long-period gratings with deposition of low-refractive-index materials," Opt. Lett., **30**, 2363-2365 (2005).
20. G. Decher, "Fuzzy Nanoassemblies: Toward Layered Polymeric Multicomposites," Science, **277**, 1232-1237 (1997).
21. J. Choi, M. F. Rubner, "Influence of the degree of Ionization on Weak Polyelectrolyte Multilayer Assembly," Macromolecules, **38**, 116-124 (2005).

1. Introduction

Long-period fiber gratings (LPFGs) consist of an index modulation of the core refractive index of a single mode fiber (SMF), with periods typically higher than 100 micron. Consequently, attenuation bands are created in the transmission spectrum at wavelengths where there is a coupling between the core and copropagating cladding modes, unlike in fiber Bragg gratings (FBGs), where there is a contrapropagative coupling between core modes. Due to this property LPFGs show an improved sensitivity to many measurands: temperature, strain, curvature and environmental refractive index [1,2]. Moreover, they can also be used in optical communications for the design of devices such as band rejection filters, equalizers and tunable filters [3-5].

The sensitivity of LPFGs to environmental parameters indicated the possibility of depositing sensitive materials on the cladding. The first experiments were developed with Langmuir Blodgett (LB) deposition technique by Rees *et al.* [6], showing that the attenuation bands shift in wavelength and that for a range of thickness values the attenuation bands vanish. Since then, it has been proved with other deposition techniques such as Electrostatic Self-Assembly Monolayer (ESAM) process [7-11] and dip-coating [12,13] the possibility of inducing resonance wavelength shifts with thin overlays.

The development of numerical methods has helped to understand the phenomena involved in these experiments. The wavelength shift of the attenuation band was explained in [14] with a scalar analysis of modes (LP mode approximation) and the application of coupled mode theory. If an overlay of higher refractive index than the cladding is deposited on this LPFG, as the overlay thickness increases, cladding modes shift their effective index to higher values. When the overlay is thick enough, one of the cladding modes is guided by the overlay. This causes a reorganization of the effective index of the rest of modes. Cladding modes with lower effective index than the one that is guided by the overlay will shift their effective index value towards the effective index of the immediate higher effective index mode. As more material is deposited, the effective index distribution before deposition is recovered. The effective index of the eighth cladding mode will be now that of the seventh one, the effective index of the seventh cladding mode will be that of the sixth mode, and so forth. A more detailed explanation of these statements can be found in earlier works [14,15]. The same is true for the resonance wavelength values, because there is a close relation between the resonance wavelength of the attenuation bands and the effective index of the cladding mode [16]:

$$\beta_{01}(\lambda) + s_0\zeta_{01,01}(\lambda) - \left(\beta_{0j}(\lambda) + s_0\zeta_{0j,0j}(\lambda)\right) = \frac{2\pi}{\Lambda} \qquad (1)$$

where β_{01} and β_{0j} are the propagation constants of the core and the j cladding modes respectively, $\varsigma_{01,01}$ and $\varsigma_{0j,0j}$ are the self-coupling coefficients of the core and the j cladding modes, s_0 is the coefficient of the first Fourier component of the grating, and Λ is the grating period.

#74595 - $15.00 USD Received 11 September 2006; revised 31 October 2006; accepted 31 October 2006

By adequate parameterization of the overlay thickness, overlay refractive index and surrounding refractive index the device could be optimized for a maximum wavelength shift , thus a maximum sensitivity, as a function of specific parameters. In [12] a refractometer is presented that improves by more than one decade the sensitivity to ambient refractive index of LPFGs without coating. In [13] a sensor for chloroform is optimized to detect low concentrations of this product.

The fading of the attenuation bands at specific overlay thickness values for both LB and ESA methods [6-8] was explained in [7,8]. It was considered that the roughness of the overlay can be interpreted as an imaginary part in the overlay refractive index. The ability of dip-coating technique to deposit low-absorption materials solves this problem at an expense of a not so accurate control of the overlay thickness [12]. However, even though the attenuation bands remain visible, the depth of the attenuation is reduced in a great manner, which does not agree with the predictions obtained with the LP mode approximation [14].

The explanation is that there is an additional cause for the fading of the attenuation bands. This was seen when a vectorial analysis of modes was used instead of the scalar one [15]. If the weak guidance condition is not satisfied, the difference in the results was not negligible. The guidance of an additional EH mode induces a modification in the cross-coupling coefficients which is also responsible for the fading of the attenuation bands. In addition to this, the modal redistribution is performed in two steps. The effective index of the eighth HE cladding mode shifts to an intermediate EH mode before it definitely shifts to the seventh HE mode. The effective index of the seventh HE cladding mode shifts to an intermediate EH mode before it definitely shifts to the sixth HE mode, and so forth. Again the same is true for the resonance wavelength values. As a result, for each transition there are two optimum overlay thickness values where a maximum wavelength shift is achieved as a function of the same variation in a parameter [15].

With both the scalar and the vectorial method it was predicted, by analyzing the effective index of modes, that the wavelength shift of the attenuation bands should occur periodically as the overlay thickness is increased [14,15]. In this work a complete analysis of the transmission spectra is presented. Both theoretical and experimental results confirm the periodicity of the phenomenon. The steepness of the second and the third transition is increased in a great manner, which could be used for the design of optical filters and for sensor purposes. Moreover, an analysis of the effect of considering two cases, first when the overlay refractive index is purely real and second with a complex component, indicates that the theoretical results predict much better the experimental ones when those theoretical results are obtained considering a complex refractive index.

In section 2 the method based on a vectorial analysis of modes and the application of coupled mode theory is used for the analysis of LPFGs coated with one overlay. The simulations of section 2 are corroborated with experimental results obtained with ESAM method in section 3. Finally, concluding remarks are presented in section 4.

2. Theory

Though in many cases the LP mode approximation permits to obtain accurate results for LPFG transmission spectra [16], the vectorial method is preferred in order to assure the rigorousness of the results [17]. That is the reason why in this work, which is focused on coated LPFGs where the weak guidance condition is met, the vectorial method is used to avoid an additional source of error. LPFGs surrounded by an infinite medium of lower refractive index than the cladding can be analyzed with a three-layer model where coupled mode theory is applied [17]. This method can be generalized for mutilayer cylindrical waveguides [18]. In [15] a four layer model has been used for the analysis of LPFGs coated with one overlay (see Fig. 1) and it will be used for the analysis performed in this work. More recently a five-layer model has been proposed for the analysis of structures with two overlays [11]. In all cases the same steps are followed. For the sake of simplicity, the structure simulated presents no azimuthal variation of the perturbed index profile after exposure to UV radiation. In this way, there is no need for a discretization of the refractive index profile and

#74595 - $15.00 USD Received 11 September 2006; revised 31 October 2006; accepted 31 October 2006

there are only interactions between the core mode HE_{11}, and HE_{1j} and EH_{1j} modes of the cladding. Once the HE and EH modes are calculated with a transfer matrix method [18], the self- and cross-coupling coefficients are obtained and they are introduced in the coupled-mode differential equations. The application of the modified phase matching condition [14] cannot be used in this case because we are interested both in the resonance wavelength and in the depth of the attenuation bands. The notation used for the cladding modes will be henceforward $HE_{1,2}$ for the first $HE_{1,j}$ cladding mode, $HE_{1,4}$ for the second $HE_{1,j}$ cladding mode, and so on; $EH_{1,3}$ for the first $EH_{1,j}$ cladding mode, $EH_{1,5}$ for the second $EH_{1,j}$ cladding mode, and so on.

The parameters used in this section correspond with those of the LPFG of the experimental part in section 3. The LPFG is composed of an SMF-28 fiber where a 320 μm period long period grating of length 25 mm has been written. In order to follow the evolution of the attenuation bands as a function of the overlay thickness, and due to the lack of information on the cladding and core refractive index as a function of wavelength after inscription of the grating, it was decided to set an initial condition that permits to fix the highest attenuation band to 1550 nm. We know that at 1310 nm the SMF-28e fiber presents a core mode effective index of 1.4677. However, this value should be modified by the inscription of the grating. In our simulation this value was set to 1.4678 and the values for the cladding and core refractive index were maintained constant in the spectrum. In addition to this, the overlay is composed of electrostatic self-assembled polyallylamine hydrochloride (PAH) and Prussian Blue (PB) as polycation, and polyacrylic acid (PAA) as polyanion. The deposition parameters used in the experimental part are detailed in section 3. According to our estimations the overlay refractive index at 1300 nm is 1.52. This value will be considered constant in the wavelength range analyzed in this work (1200 to 1600 nm). The dispersion of the overlay refractive index should play a role in the results presented henceforward. However, the influence of the overlay thickness increase plays a more important role. Consequently, there is a correspondence between the theoretical and the experimental results. The surrounding index is water (refractive index 1.33).

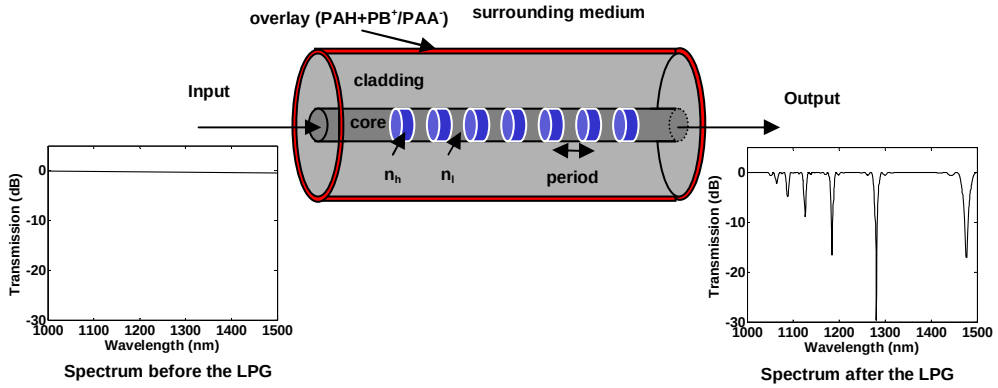

Fig. 1. LPFG coated with one overlay.

In Fig. 2 it is shown the wavelength shift of the attenuation bands (regions of lower transmitted power) as a function of the overlay thickness (0 to 5000 nm), by considering that the refractive index of the overlay is purely real. The phenomenon is periodic and repeats three times without a decrease in the attenuation band depth. The most interesting point is that the transition is more abrupt in the second and the third transition. The cause is that the periodical guidance of modes as a function of the overlay is retarded for higher wavelengths. Moreover, for the third transition the slope is nearly infinite in the $HE_{1,14}$ band, which moves from 1375 nm to 1285 nm, and negative for the $HE_{1,16}$ band, which moves from 1550 nm to 1375 nm.

#74595 - $15.00 USD Received 11 September 2006; revised 31 October 2006; accepted 31 October 2006

On the one hand, if an infinite slope is obtained in the wavelength shift of the attenuation bands, wide filters can be designed. This is the case in one of the bands of the third transition in Fig. 2. The transmission spectrum for an overlay of 3780 nm is represented in Fig. 3a, where a wide optical filter of 56.6 nm is obtained for the $HE_{1,14}$ cladding mode resonance. In fact the slope is not exactly infinite. That is the reason why it seems that the filter is the combination of two attenuation bands. The stability of the filter can be affected by parameters such as temperature. However, if a second overlay of lower refractive index than the cladding is deposited the stability can be improved [19]. On the other hand, if the slope of transition of the attenuation bands (Fig. 2) is negative then there can be more than one resonance wavelengths for the same cladding mode, which could have application in multiparameter sensing. This phenomenon can be observed in Fig. 3b where the transmission spectrum for an overlay of 4120 nm is presented. Since the slope of the transition is negative there are three resonance wavelengths for the same $HE_{1,16}$ mode instead of one. These points are located at 1406, 1470 and 1514 nm.

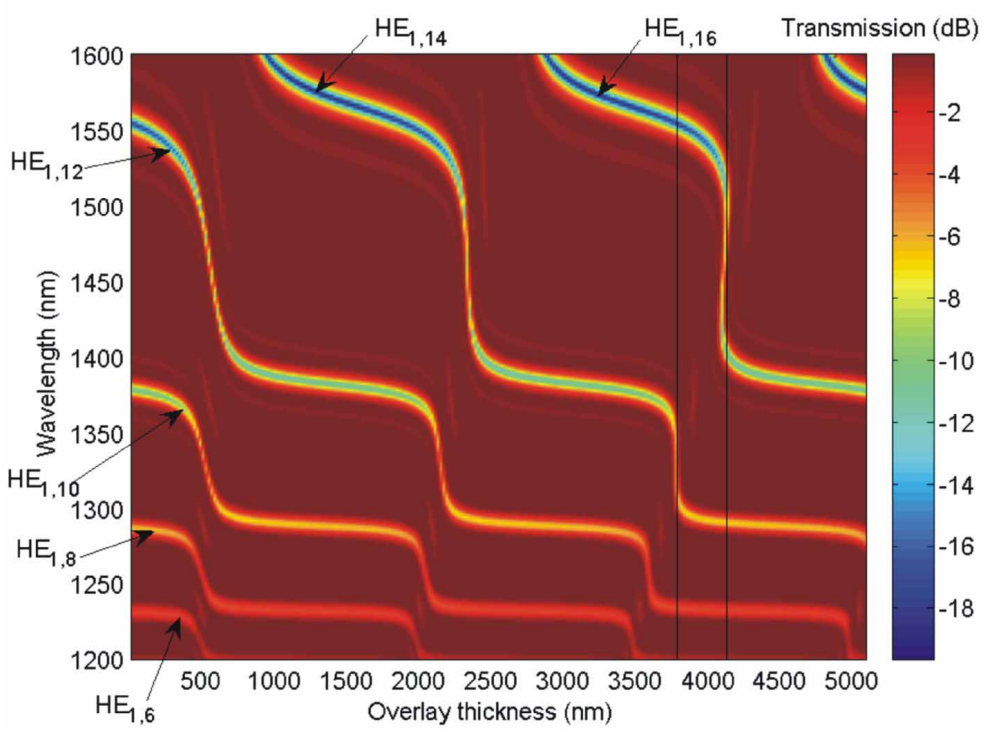

Fig. 2. Spectrum as a function of the overlay thickness (simulation). Overlay index 1.52. Surrounding medium: water.

It is well known that some materials deposited using ESA method may present a not negligible roughness. This roughness can be interpreted as a complex refractive index [7, 8]. To this purpose, the same analysis of Fig. 2 is performed with the exception that the overlay refractive index is 1.52 + 0.0025i and that the range of overlay thickness values analyzed is now 0 to 3800 nm. Two cases are considered for this analysis: first, when the surrounding medium is water (see Fig. 4) and second, when the surrounding medium is air (see Fig. 5), which are the same conditions of the experiments performed in section 3.

#74595 - $15.00 USD Received 11 September 2006; revised 31 October 2006; accepted 31 October 2006

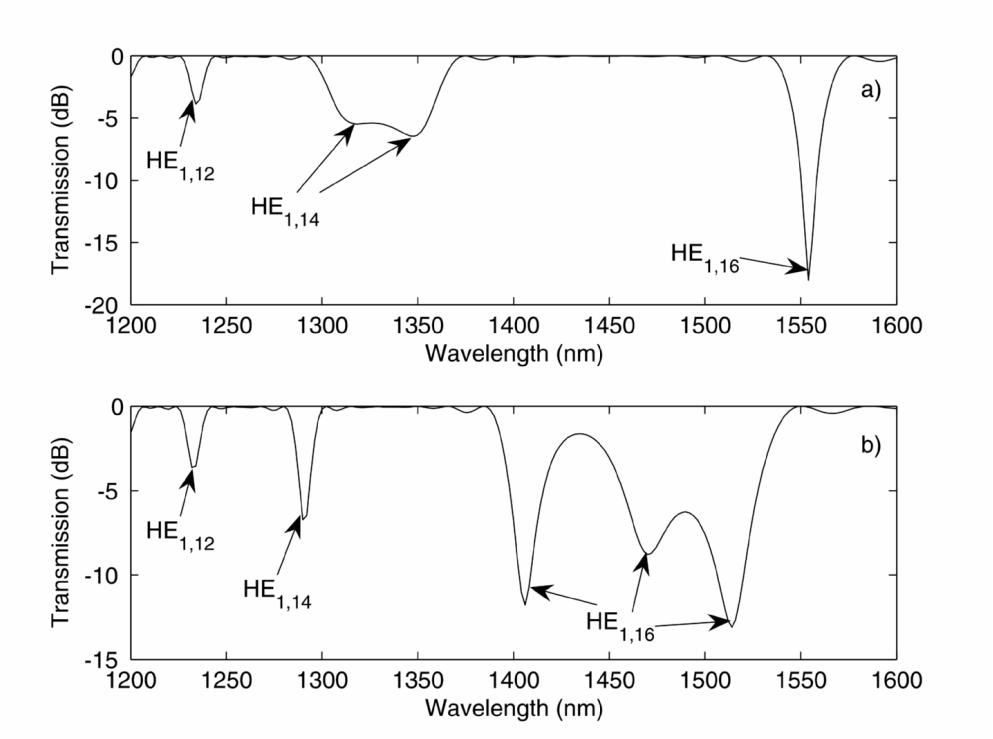

Fig. 3. Transmission spectrum (simulation) for two overlay thickness values: a) 3780 nm; b) 4120 nm. Overlay index 1.52. Surrounding medium: water.

The main difference in the results is a fading of the attenuation bands in the transition region, which is more important in the second transition of Fig. 4. Due to the fading of the attenuation bands in the second transition, it is difficult to assert whether the attenuation band shifts towards the immediate lower-order attenuation band. For the band located at 1550 nm it is clear that it shifts to the one situated at 1375 nm. However, for the lowest-order band this fact is not so clear. In fact, it was proved in [8] that when an LPFG is coated with one overlay of complex refractive index it is not always the lowest order-mode which is guided in the overlay. As a result the attenuation bands can be subdivided into two groups that shift in a different way. The first group is composed of the bands induced by cladding modes of higher-order than the one guided in the overlay. These bands shift to the immediate lower-order bands. The second group is composed of the attenuation bands of lower order than the guided mode. These bands originally shift to the immediate lower-order band (blue shift). Once a mode is guided in the overlay they experiment a red shift to their original position (uncoated LPFG spectrum). In the third transition this fact is more evident. The fading is more important, and it resembles that the lowest order band does not shift to the immediate lower band but to itself. After an initial blue shift, there is a final red shift. If the overlay is lossless, as it is the case analyzed in Fig. 2, the guided mode is the lowest-order mode. In this case there are only attenuation bands that belong to the first group. Consequently, all of them shift to the immediate lower order attenuation band.

#74595 - $15.00 USD Received 11 September 2006; revised 31 October 2006; accepted 31 October 2006

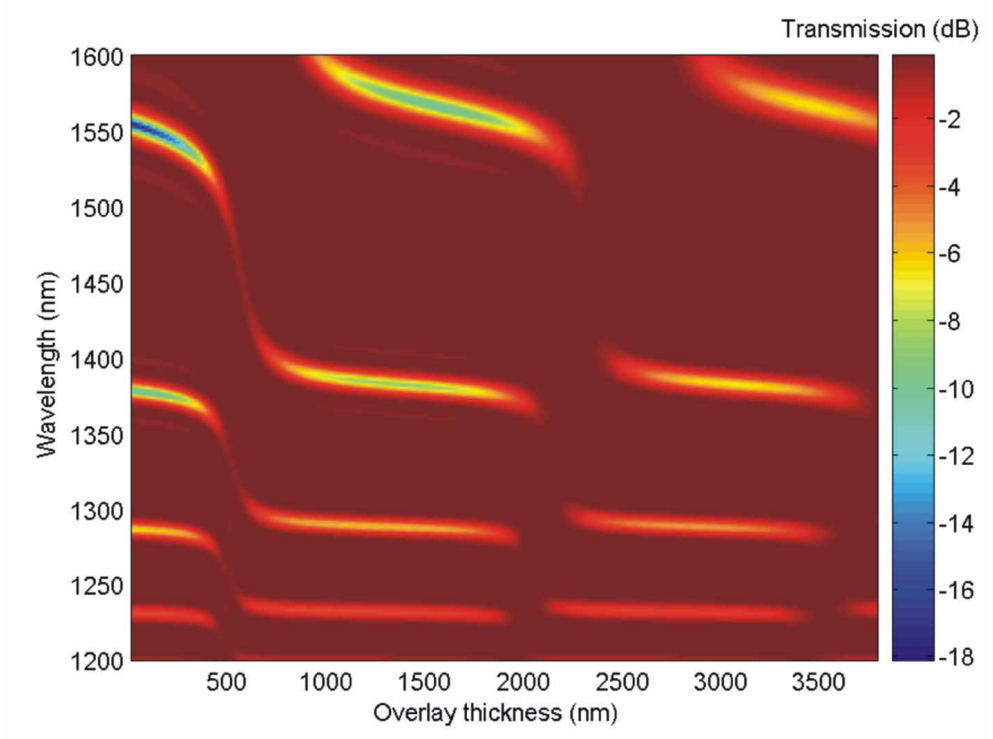

Fig. 4. Spectrum as a function of the overlay thickness (simulation). Overlay index 1.52+0.0025i. Surrounding medium: water.

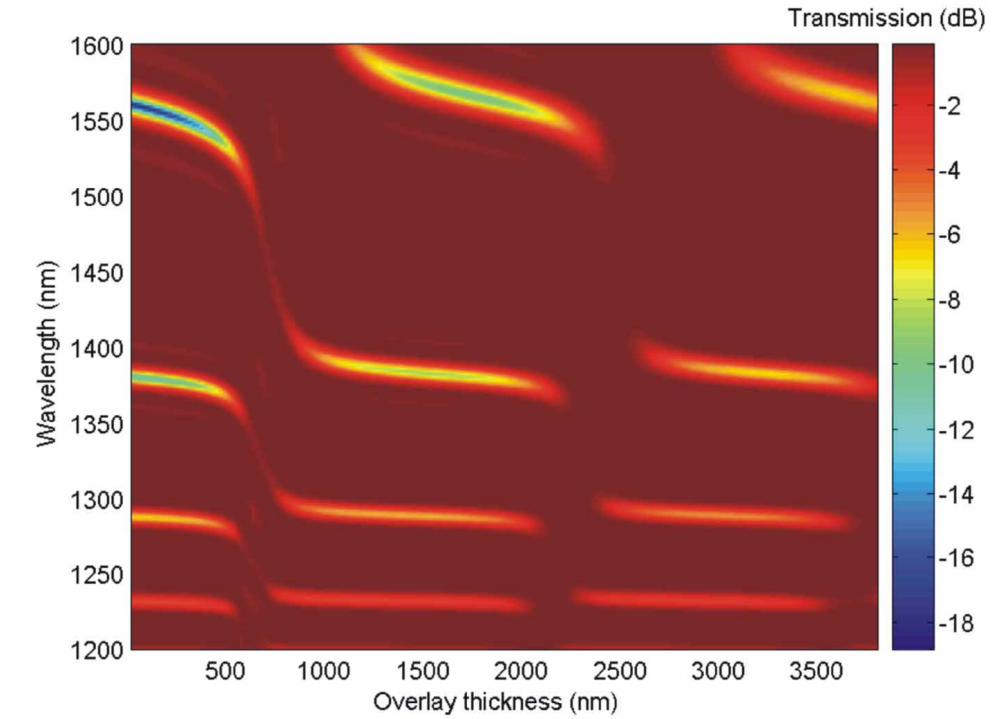

Fig. 5. Spectrum as a function of the overlay thickness (simulation). Overlay index 1.52+0.0025i. Surrounding medium: air.

#74595 - $15.00 USD Received 11 September 2006; revised 31 October 2006; accepted 31 October 2006

In Fig. 5 the results obtained in air are presented, which are similar to those obtained in Fig. 4 with two exceptions. First, the transitions occur for higher thickness values. The explanation is that the guidance of a mode in the overlay occurs later due to the more asymmetric refractive index distribution at both sides of the overlay [14]. The asymmetric distribution is considered as the contrast between the indices of the two media that surround the overlay. If the surrounding medium is air the contrast with the cladding is higher than in the case where the surrounding medium is water. The second difference is that attenuation bands induced by EH modes that are not visible when the LPFG is uncoated, appear in the transition region in-between the main attenuation bands. If the LPFG is surrounded with water, the refractive index distribution is more symmetric. As a result, it approaches more the weak guidance condition, where no EH modes appear. However, if the surrounding medium is air the structure is more asymmetric and the EH modes are visible [15].

3. Experimental results

In this section the theoretical results are corroborated with experimental ones performed with ESA method. This technique is used to build up coatings on a variety of different substrate materials such as ceramics, metals, and polymers of different shapes and forms, including planar substrates, prisms, and convex and concave surfaces. The method is based on the construction of molecular multilayers by the electrostatic attraction between oppositely charged polyelectrolytes in each monolayer deposited, and involves several steps [20]. It avoids the necessity of a dust-free atmosphere to perform the experiments and its accuracy permits to obtain bilayer thickness values ranging between 0.5 and 15 nm [21]. The thickness depends on parameters such as the pH of the solutions, the immersion time and the temperature.

The deposition parameters are: polyallylamine hydrocholoride (PAH) (obtained from Aldrich - average MW 70000): 0.935 g/L (2 thirds) + Prussian Blue soluble (PB) (obtained from Riedel-de Haën AG): 1.25 g/L (1 third) for the polycation, and for the polyanion polyacrylic acid (PAA): 50 ml/L (the base solution was obtained from Aldrich - 40 wt. % in water and average MW 30000). The pH of the solutions is 4.5.

The most direct method to analyze the spectral evolution as the LPFG is coated with an overlay consists of illuminating the grating with a broadband light source (Agilent 83437A) and capturing the transmitted light with an optical spectrum analyzer (Agilent 86142A). In this way it will be obtained a spectrum with attenuation bands generated by the power absorbed by the cladding modes (see Fig. 1).

In Fig. 6 it is shown the wavelength shift of the attenuation bands (regions of lower transmitted power) as a function of the number of monolayers. The measures are taken when the device is immersed in water. The experimental results obtained in Fig. 6 agree much better with the theoretical results of Fig. 4 than those of Fig. 2. In the first transition there is a partial fading whereas in the second one there is a complete fading. By fitting both figures, the monolayer overlay thickness can be estimated as 20 nm.

It is important to note that the fading is negative in terms of application of the properties observed in section 2. The fading is caused by the imaginary part in the refractive index of the ESA material used. The reason why this lossy material was used is that its wide monolayer thickness permitted to study three transitions with only 190 monolayers. This should be avoided by using less absorptive materials.

As an example, the effect of the incremental coating of the LPFG in the evolution of the spectra of Fig. 6 is also presented in Fig. 7 for two transitions. In the first transition, for 25 monolayers the bands are shifted leftwards. For 45 monolayers the bands are approaching the immediate lower-order band. However, for the second transition the phenomenon is more abrupt. It occurs between the monolayer 118 and the monolayer 128. A movie can be visualized in an .avi file.

#74595 - $15.00 USD Received 11 September 2006; revised 31 October 2006; accepted 31 October 2006

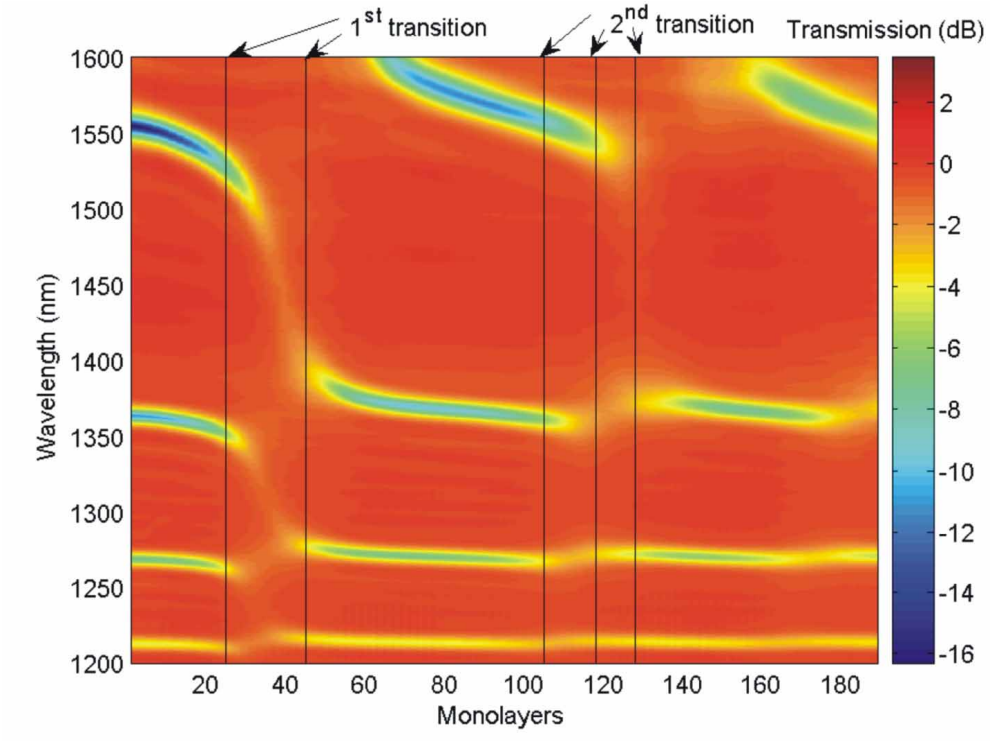

Fig. 6. Spectrum as a function of the overlay thickness (experiment). Overlay index 1.52+0.0025i. Surrounding medium: water.

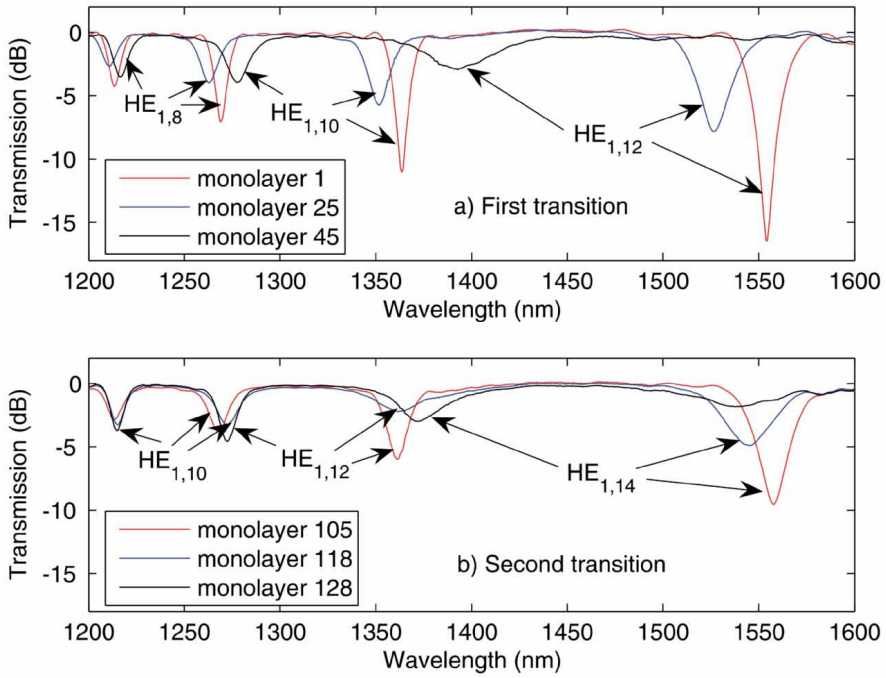

Fig. 7. Transmission spectra for the first and the second transition of modes. The movie of the transitions can be seen in an avi file.

#74595 - $15.00 USD Received 11 September 2006; revised 31 October 2006; accepted 31 October 2006

In Fig. 8 the results obtained in air are presented, which are similar to those obtained in Fig. 5 with the same particularities: the transitions take place later as predicted in [14], and the attenuation bands induced by EH modes, which are not visible when the LPFG is uncoated, appear in the transition region in-between the main attenuation bands. The reason is the more asymmetric refractive index distribution. The weak guidance condition is better approached in case the surrounding medium is water

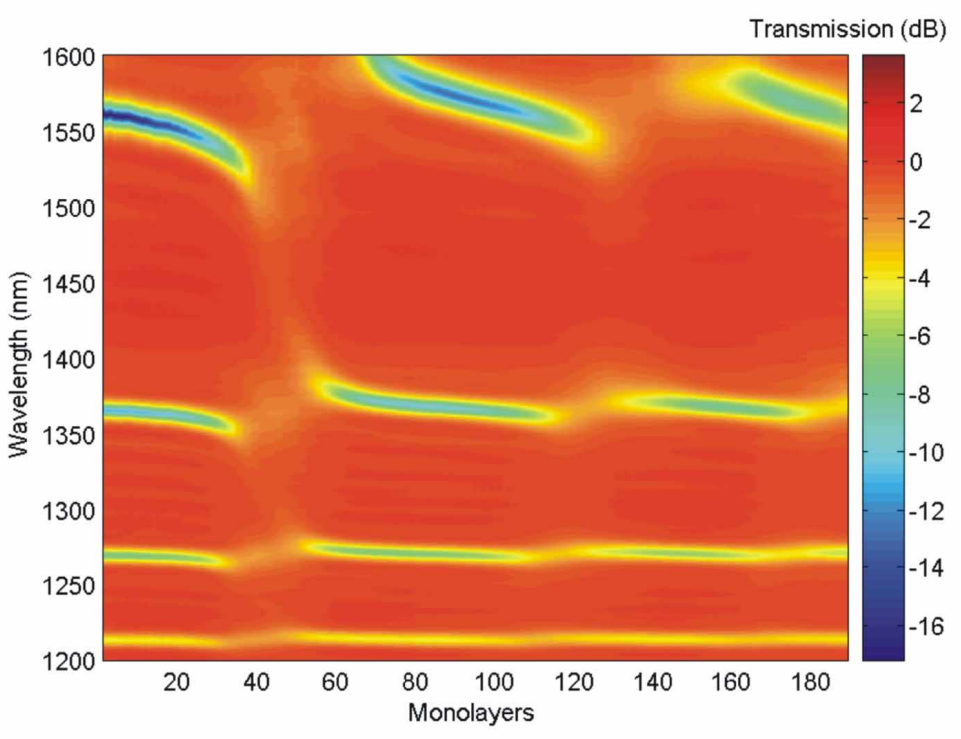

Fig. 8 Spectrum as a function of the overlay thickness (experiment). Overlay index 1.52+0.0025i. Surrounding medium: air.

4. Conclusions

In this work it has been proved both theoretically and experimentally that the periodic effective index redistribution analyzed in [14,15] for LPFGs coated with an overlay of higher refractive index than the cladding is also periodic for the transmission spectrum. However, the shape of the resonance wavelength shift is different depending on the overlay thickness. This could be used for the design of wide band filters and sensor purposes. The case of overlays with a complex refractive index has been also theoretically analyzed and corroborated experimentally for different surrounding medium conditions.

Acknowledgments

This work was supported by Spanish Ministerio de Ciencia y Tecnologia and FEDER Research Grants CICYT-TIC 2004-05936-C02-01/MIC, Gobierno de Navarra and FPU MECD Grant.

#74595 - $15.00 USD Received 11 September 2006; revised 31 October 2006; accepted 31 October 2006